Multisensor Studies on El Niño-Southern Oscillations and Variabilities in Equatorial Pacific

Xiao-Hai Yan, Yun He, W. Timothy Liu, and R. Dwi Susanto

Abstract

The variabilities of the western Pacific warm pool including areas, positions of gravitatioal center, sea surface temperature anomaly, sea surface height anomaly are studied using Florida State University wind, ERS-1, 2, and NSCAT scatterometer wind; Reynolds optimum interpolation and historical reconstructed sea surface temperature data; and TOPEX/Poseidon sea surface height data. The relations between the westerly wind forcing and corresponding sea surface height and sea surface temperature responses in the tropical Pacific Ocean during El Niño and other years are analyzed. A common characteristic for typical El Niño events is found and is explained by the westerly wind pattern. Time-frequency analysis of the Topex/Poseiden data time series along the equator using the Empirical Model Decomposition-Hilbert Spectrum method is also performed.

1 Introduction

The El Niño-Southern Oscillation (ENSO) phenomenon and associated disruption of the ocean/atmosphere systems in the tropical Pacific Ocean can have enormous global economic and social impacts: It may cause drought, wildfires, severe cyclones, severe storms, and floodings all over the world. For example, the economic damage of the unusually strong El Niño of 1982-83 was as large as 1.1 billion dollars in the Mountain and Pacific States of the United States alone. A better understanding of the oceanic and atmospheric processes involved in this phenomenon may improve our ability to predict the occurrence and effects of El Niño, thus potentially saving lives, property, and reducing damage costs on a large scale.

On average, El Niño events occur at a 4-7-year interval, with strong events occurring about once a decade (Philander, 1990). Recent El Niño events seem to be much stronger and frequent than usual. Just three years after the persistent warm conditions in 1991-94 ended, the latest 1997-98 El Niño, appeared with a strength as great as that of the 1982-83 event, one of the strongest El Niños ever observed.

The existence of westerly wind bursts (WWBs) is one of the major climatic characteristics of the Western Tropical Pacific Ocean (WTPO). In this paper, WTPO is defined as the region from 20°S to 20°N, and from 120°E to 150°W. WWBs are potentially important as triggering mechanisms for ENSO events through the anomalous zonal stress that they place on the equatorial ocean (Lukas and Lindstrom, 1991). WWBs cause warm water to spread over the Pacific with a consequent sea surface temperature (SST) and sea surface height (SSH) increase as well as a sea surface pressure decrease in the eastern Pacific.

From the description of El Niño, it is seen that El Niño can be determined from SST anomaly, wind stress, and sea surface height anomaly (SSHA) composites. In this paper, atmospheric forcing

and ocean surface responses are studied in terms of westerly wind, SST data, SSH data and the relationships among them. To do so, satellite data from ERS-1, ERS-2 and NSCAT scatterometer along with Florida State University (FSU) wind data are used to parameterize the total westerly wind forcing (TWWF) in the WTPO. The TWWF is obtained by integrating the total westerly wind stress in the WTPO with the corresponding area. Reynolds optimum interpolation sea surface temperature (OISST) (Reynolds and Smith, 1994) and reconstructed historical SST (Smith *et al.*, 1996) are used to measure WPWP area, centroid (or gravitational center), and SST anomaly in the Niño3.4 region (5°N - 5°S, 170°W - 120°W, where SST anomaly in this region could be used to quantitatively define the El Niño strength (Trenberth, 1997)). Observed southern oscillation index (SOI) standardized data are also used. SOI is the sea level pressure difference anomaly between stations at Tahiti and Darwin, Australia. TOPEX/Poseidon data are used to calculate the SSHA and in the time-frequency analysis of equatorial wave signals.

2 Westerly Wind Forcing and SST Response

In this section, we would like to study how SST related parameters respond to the westerly wind forcing. Figure 1 shows the TWWF in the WTPO and the western Pacific warm pool (WPWP) area, centroid, SST anomaly in the Niño 3.4 region, and negative SOI from January 1982 to March 1998 after removing the annual cycle (except for the meridional component of the WPWP centroid movement, which has a highly annual cycle due to the annual solar radiation cycle). Here WPWP is defined as the area with SST greater than 28°C within the region of 30°S-30°N, 120°E-110°W. And the WPWP centroid is defined as the two-dimensional gravitational center of the WPWP (Ho *et al.*, 1995; Yan *et al.*, 1992, 1997). Table 1 shows the correlation coefficients with confidence intervals at 95% confidence level and the phase lags between these parameters. The results show that besides the SST anomaly in the Niño 3.4 region and the SOI, the WPWP area and the longitude of the centroid can be very good indexes for El Niño events too.

Based on 10 years of NOAA satellite multi-channel sea surface temperature (MCSST) data from 1982 to 1991, Ho *et al.* (1995) observed that during the year of an El Niño onset (years 1982 and 1986) in this ten year period, the WPWP centroid moves clockwise as opposed to counterclockwise during other years. Yan *et al.* (1997) argued that the 1991-93 El Niño was somewhat different from the previous two events with regards to the direction of the WPWP centroid movement, which is counterclockwise during the 1991-93 event.

We would like to know if the 1997-98 event and the other El Nino events have the characteristic reported by Ho *et al.* (1995), or it behaves similar to 1991-93 event. In order to do this, we have tracked the phenomenon from January 1950 to March 1998 by using Reynolds reconstructed SST from historical data. We found most El Niño events in the past 50 years (nine out of ten) have shown this common characteristic; i.e., the WPWP centroid moves clockwise during the year of El Niño onset while it moves counterclockwise during other years. Here when we talk about the direction of movement, we use the interior of the WPWP centroid trajectory as reference. Some typical events include: 1965-66, 1972-73, 1982-83, 1986-87, and 1997-98. An illustrative diagram of the WPWP centroid movement is shown in Figure 2.

By checking the corresponding TWWF (Figure 3), one can see that most of these El Niño

Table 1: Correlation coefficients with the confidence intervals at 95% significance level and the Phase Lags (in month, positive means the parameter in the left column leads the parameter in the right row) between the TWWF in the WTPO and the WPWP related parameters.

Parameters		TWWF	WP_Area	Cen_Lon	SST_Anom	-SOI
TWWF	corr	-	0.67 ± 0.19	0.76 ± 0.15	0.84 ± 0.11	0.70 ± 0.18
	lag	-	4	5	4	5
WP_Area	corr	-	-	0.91 ± 0.07	0.90 ± 0.07	0.94 ± 0.04
	lag	-	-	0	0	0
Cen_Lon	corr	-	-	-	0.97 ± 0.02	0.94 ± 0.04
	lag	-	-	-	0	0
SST_Anom	corr	-	-	-	-	0.92 ± 0.06
	lag	-	-	-	-	1

events have some common characteristics: Westerly wind forcing increases during the first half year of El Niño onset causing western Pacific warm water to migrate eastward. This is associated with the seasonal northward movement of the WPWP centroid during the second and third quarters of the year. Following this, westerly wind forcing decreases during the second half of the year, while the WPWP continues to expand eastward for several more months since the ocean adjusts to atmospheric changes slowly and has a "memory" of earlier winds (Philander, 1998). Finally, the WPWP centroid will retreat westward while TWWF declines. This movement is associated with the seasonal southward movement of the WPWP centroid during the fourth and first quarters of the year. The whole scenario defines the clockwise movement of the WPWP centroid. It also defines the orientation of the major axis of the WPWP centroid movement ellipsoid to be southwest-northeastward. It should be pointed out that the continuing eastward movement after the westerly wind decreases is critical in determining the clockwise movement of the WPWP centroid.

As for the other years and the onset year of the 1991-93 El Niño, we find the opposite story: Westerly wind forcing decreases during the first half of the year and increases during the second half of the year. The WPWP centroid moves northwestward first and then southwestward in between for several months, and finally southeastward, completing a counterclockwise movement. The major axis of the orientation of the WPWP centroid movement ellipsoid is southeast-northwestward.

3 Westerly Wind Forcing and Sea Surface Height Response

Sea surface height response to westerly wind forcing is studied in this section. Figure 4 shows the TWWF in the WTPO and the SSHA in the equatorial Pacific basin from October 1992 to March 1998, respectively. Examples of SSHAs in the equatorial Pacific basin are shown in Figures 4b and 4c. The correlation coefficient between the TWWF in the WTPO (Figure 4a) and the SSHA at 168°E (Figure 4b) is -0.15 ± 0.35, and that with the SSHA at 144°W (Figure 4c) is 0.90 ± 0.09 at 95% significance level. The result agrees well with Kessler *et al.* (1995) at two similar locations in the western and eastern basins. Besides these two specific longitudes, the correlation coefficients and phase lags between the TWWF and the SSHA along the equator at different longitudes from 120°E to 80°W are calculated in this study and shown in Figures 4d and 4e. The correlation coefficients are high in the eastern basin, but low in the western basin. The phase lag is zero in the western basin and one month in the eastern basin. One could also see a boundary between the western and eastern basins at approximately 150°W. This is the average location of the WPWP eastern boundary at the equator. The westerly wind anomaly is highly correlated with SSHA in the eastern basin implies that the equatorial Kelvin waves in the central and eastern basins are remotely forced by the westerly wind in the western basin.

4 Time-Frequency Analysis

Note: put Dwi's part here for overall balance and contents consistency. So, his figure will be Figure 5.

5 Conclusion and Discussion

From the above analyses, it is seen that the TWWF is closely related to the sea surface height and sea surface temperature anomalies. WPWP Area and longitude of the centroid could be used as El Niño indexes. A common characteristic for typical El Niño events is also found: the WPWP centroid moves clockwise during a year of El Niño onset, with the major axis facing southwest-northeastward, while the centroid moves counterclockwise during other years, and the major axis faces southeast-northwestward. It could be explained by the TWWF wind patterns.

The contrast between the 1991-93 and other El Niño events may be due to the differences in magnitude of the El Niño-related wind pattern shifts in the WTPO before and during the events and the seasonal phase-lock of the ENSO events (Yan *et al.*, 1997). That is, for a typical El Niño event, the warm phase of El Niño (eastward displacement) started in the second and third quarters associating with the northward seasonal migration, the trajectories were clockwise. For 1991-1993, however, the El Niño related eastward motions started in the last and first quarters associating with the northward seasonal migration (small and unusual events), the centroid trajectories were counterclockwise.

TWWF in the WTPO is highly correlated with the SSHA in the eastern basin of the tropic Pacific Ocean, but not correlated with that in the western basin. Equatorial Kelvin waves are remotely forced by the westerly winds in the WTPO.

Note: Add conclusions for Dwi's part.

Acknowledgment

This research is supported partially by the National Science Foundation and by the Earth Observing System (EOS) Interdisciplinary Science investigation of the National Aeronautics and Space Administration.

References

NOTE: add Dwi's references.

Ho, C.-R., X.-H. Yan, and Q. Zheng, 1995. Satellite observation of upper-layer variabilities in the Western Pacific Warm Pool. *Bulletin of the American Meteor. Soc.*, 76 (5), 669-679.

Huang, N., S. Long, and Z. Shen, 1996. The mechanism for frequency downshift in nonlinear wave evolution. em Adv. Appl. Mech., 32, 59-111.

Kessler, W. S., M. J. McPhaden, and K. M. Weickman, 1995. Forcing of intraseasonal Kelvin waves in the equatorial Pacific. *J. Geophys. Res.* 100, 10,613-10,631.

Kinsman, B. , 1965. *Wind Waves*. Prentice-Hall, New Jersey.

Lukas, R. and E. Lindstrom, 1991. The mixed layer of the western equatorial Pacific Ocean. *J. Geophys., Res.*, 96, Suppl., 3343-3357.

Philander, S. G. H., 1990. *El Niño, La Niña, and the Southern Oscillation*. Academic Press Inc., New York, 293pp.

Philander, S. G., 1998. *Is the Temperature Rising? The Uncertain Science of Global Warming*. Princeton Univ. Press, Princeton, NJ, 262pp.

Reynolds, R. W. and T. M. Smith, 1994. Improved global sea surface temperature analysis using optimum interpolation. *J. Clim.*, 7 (6), 929-948.

Smith, T. M., R. W. Reynolds, R. E. Livezey, and D. C. Stokes, 1996. Reconstructions of historical sea surface temperatures using empirical orthogonal functions. *J. Clim.*, 9 (6), 1403-1420.

Trenberth, K. E., 1997. Definitions of El Niño. *Bull. Amer. Meteor. Soc.*, 78 (12), 2771-2777.

Yan, X.-H., C.-R. Ho, Q. Zheng, and V. Klemas, 1992. Temperature and size variabilities of the western Pacific warm pool. *Science*, 258, 1643-1645.

Yan, X.-H., Y. He, W. T. Liu, Q. Zheng, and C.-R. Ho, 1997. Centroid motion of the western Pacific warm pool in the three recent El Niño-Southern Oscillation events. *J. Phys. Oceanogr.*, 27 (No. 5), 837-845.

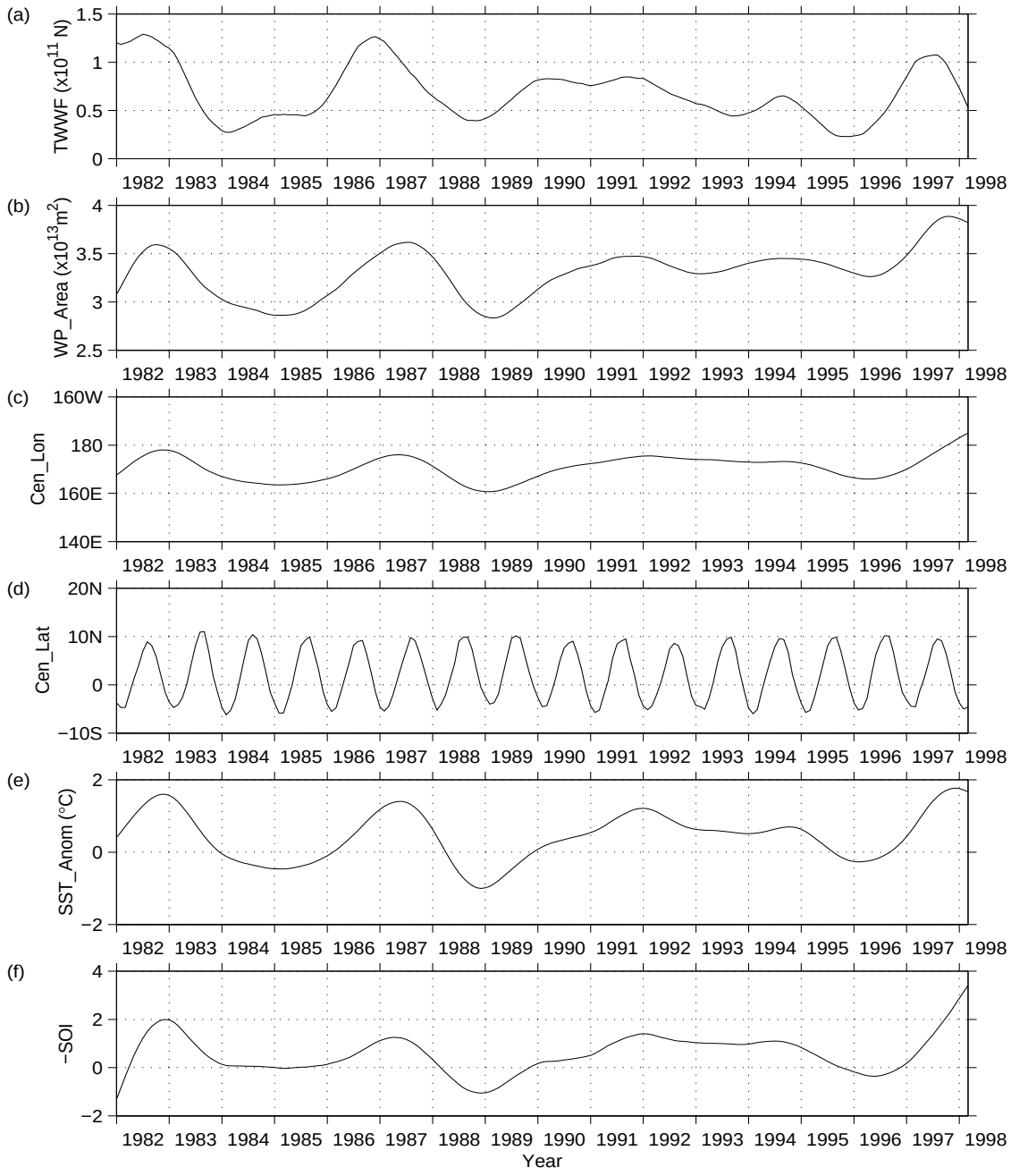

Figure 1: Relationship between the TWWF and SST related parameters after removing the annual cycle. From January 1982 to March 1998: (a) The TWWF in the WTPO; (b) the WPWP area; (c) the longitude of the WPWP centroid; (d) the residue of the meridional component of the WPWP centroid after removing the seasonal cycle; (e) the SST anomaly in the Niño 3.4 region; (f) negative SOI.

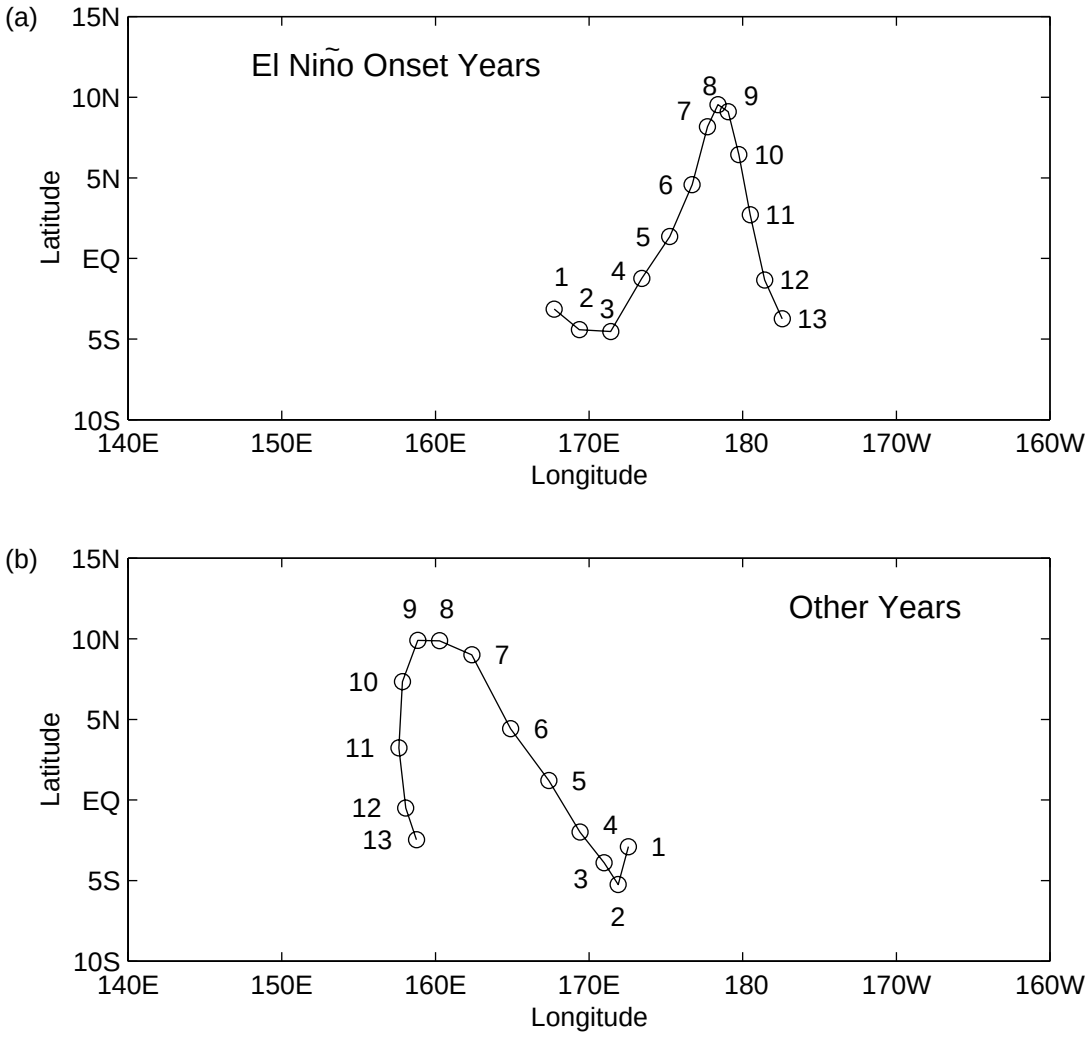

Figure 2: An illustrative of the WPWP centroid movement. (a) It moves clockwise with the major axis facing southwest-northeastward during onset of a typical El Niño year (shown in this figure: year 1983); (b) it moves counterclockwise with the major axis facing southeast-northwestward during other years (shown in this figure: year 1988). Small circles represent the monthly averages of the WPWP centroids location; numbers from 1 to 12 stand for January to December each year, and 13 stands for January next year.

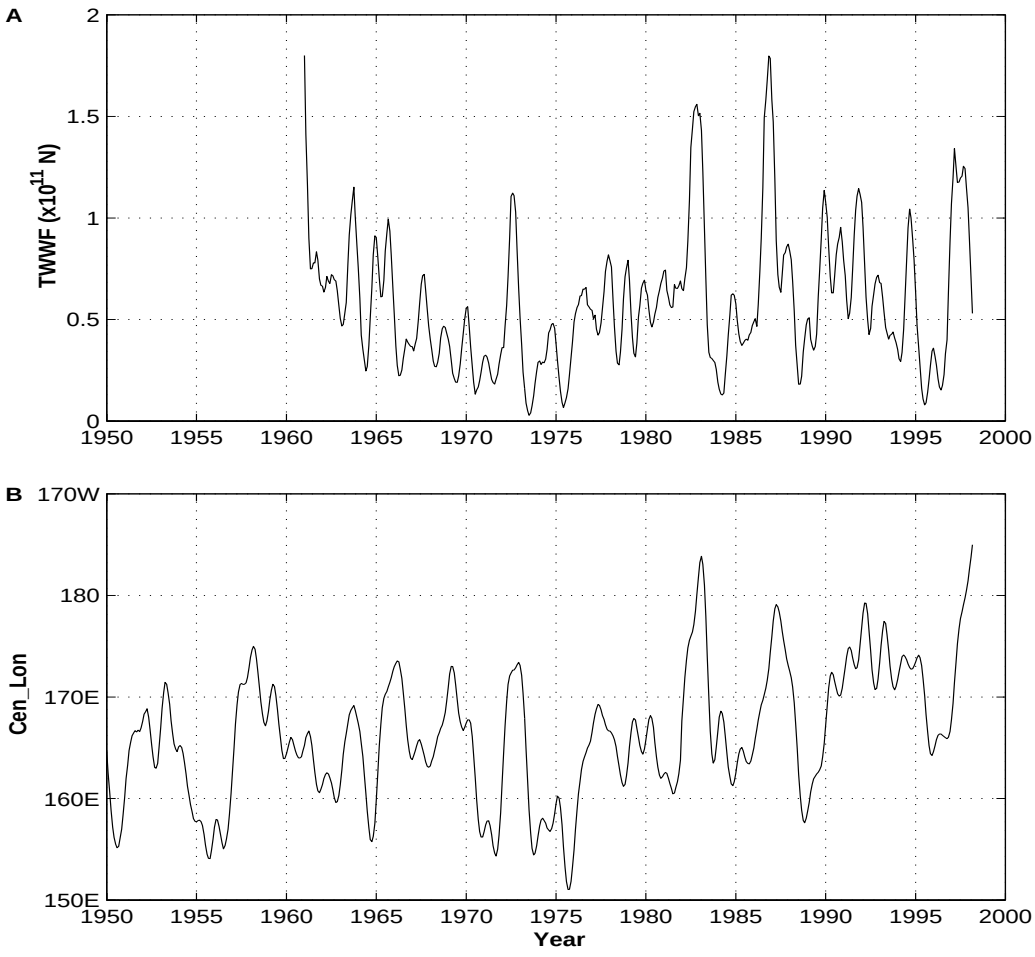

Figure 3: (A) The TWWF in the WTPO from January 1961 to March 1998; (B) The longitude of the WPWP centroid from January 1950 to March 1998.

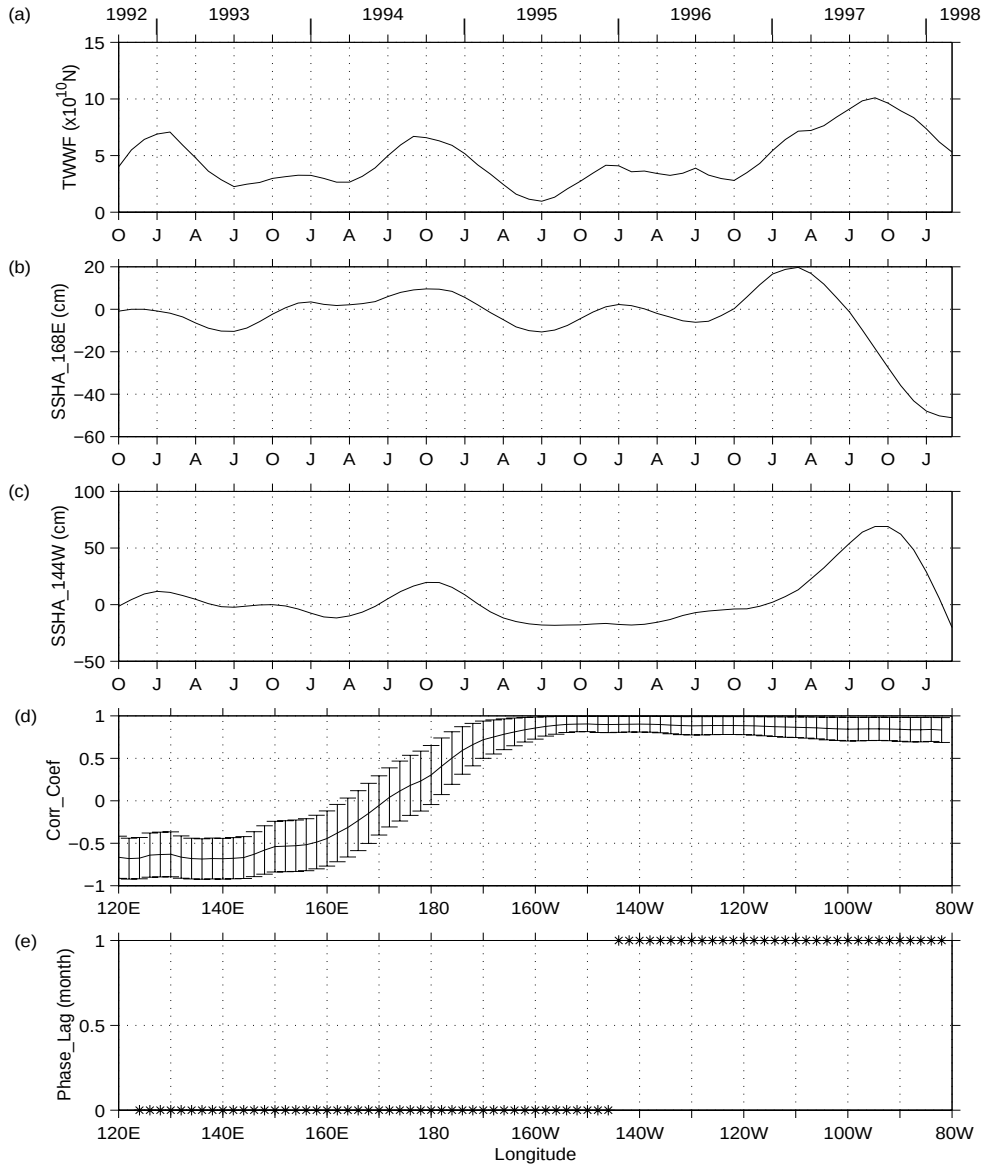

Figure 4: Relationship between the TWWF in the WTPO and the SSHA. From October 1992 to March 1998: (a) the TWWF in the WTPO; (b) the SSHA at the equator at 168°E; (c) the SSHA at the equator at 144°W; (d) correlation coefficients and confidence intervals at 95% significance level between the TWWF in the WTPO and SSHA along the equator at different longitudes; (e) phase lags between the TWWF in the WTPO and the SSHA along the equator at different longitudes for maximum correlation.